ELSEVIER

Journal of Photochemistry and Photobiology A: Chemistry 101 (1996) 251–255

Journal of PHOTOCHEMISTRY AND PHOTOBIOLOGY A:CHEMISTRY

Titanium dioxide-photocatalysed decomposition of some thiocarbamates in water

Michela Sturini [a], Elisa Fasani [a], Cristina Prandi [b], Adele Casaschi [a], Angelo Albini [a,*]

[a] *Department of Organic Chemistry, University of Pavia, via Taramelli 10, 27100 Pavia, Italy*

[b] *Department of Organic and Applied Chemistry, The University, via Giuria 7, 10125 Torino, Italy*

Received 28 March 1996; accepted 28 May 1996

Abstract

Irradiation of both aliphatic and aromatic thiocarbamate herbicides in an aqueous suspension of titanium dioxide leads to their efficient decomposition (maximum quantum yield up to 0.12 for the aliphatic derivatives, lower for the aromatic derivatives). The process involves the surface-adsorbed substrate, and is initiated through hydrogen abstraction by the hydroxyl radical from the *N*-alkyl chain (not from the *S*-alkyl chain unless this is a benzyl group) as indicated by the characterization of the main degradation intermediates.

Keywords: Photocatalysed decomposition; Thiocarbamates; Titanium dioxide; Water purification

1. Introduction

Thiocarbamates are one of the most largely used families of herbicides. As a consequence, their presence in agricultural effluents is a serious problem. Solar light [1] and, more effectively, UV light [2,3] have been shown to improve the oxidative degradation of some of these compounds in natural water. The addition of hydrogen peroxide greatly accelerates the photodecomposition [4,5]. There are also indications that semiconductor photo-oxidants, such as titanium dioxide or zinc oxide, can be used for the oxidative degradation of some compounds of this class [6].

The last method has several potential advantages. As an example, titanium dioxide is an inexpensive, non-toxic material which has convenient absorption properties, making it suitable for use with solar light. Its application for water purification is promising [7–12]. However, before heterogeneous photosensitization can be proposed as a general and trouble-free method, it is required that the chemistry of various classes of pollutants under these conditions is known in detail. In order to contribute towards this aim, we carried out laboratory tests with some thiocarbamate herbicides to obtain a better understanding of the characteristics of the processes involved. This was performed under conditions of low absorbed flux, so that the results are predictive of the degradation in solar light.

* Corresponding author.

1010-6030/96/$15.00 © 1996 Elsevier Science S.A. All rights reserved
PII S1010-6030(96)04408-5

2. Results

The investigation was carried out on two aliphatic thiocarbamates, namely Molinate (**1**), the *S*-ethyl ester of 1-*H*-hexahydroazepine-1-carbothioic acid, and Eptam (**2**), the *S*-ethyl ester of *N*,*N*-dipropylcarbamothioic acid, and two aromatic thiocarbamates, namely Tiocarbazil (**3**), the *S*-phenylmethyl ester of *N*,*N*-bis-(1-methylpropyl)-carbamothioic acid, and Thiobencarb (**4**), the *S*-(4-chlorophenylmethyl) ester of *N*,*N*-diethylcarbamothioic acid (Table 1, Scheme 1).

Air-equilibrated aqueous suspensions (10 ml) of titanium dioxide (Degussa P25), to which 10–200 ppm of the substrates had been added, were first stirred in order to allow adsorption equilibrium to be reached and were then irradiated at 340–380 nm. Under these conditions, all the starting materials were effectively degraded within 2 h (see Fig. 1 and Fig. 2). Unirradiated controls were inactive, nor was any

Table 1
Products formed on heterogeneous photosensitization of thiocarbamates **1–4** evaluated at approximately 50% conversion of the starting substrate

Substrate	Products (% on the converted substrate)
1	**5** (22), **6** (5)
2	**7** (6), **8** (6), **9** (5)
3	**10** (2)
4	**11** (1), **12** (2)

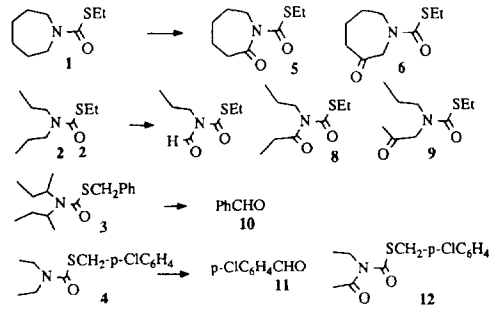

Scheme 1.

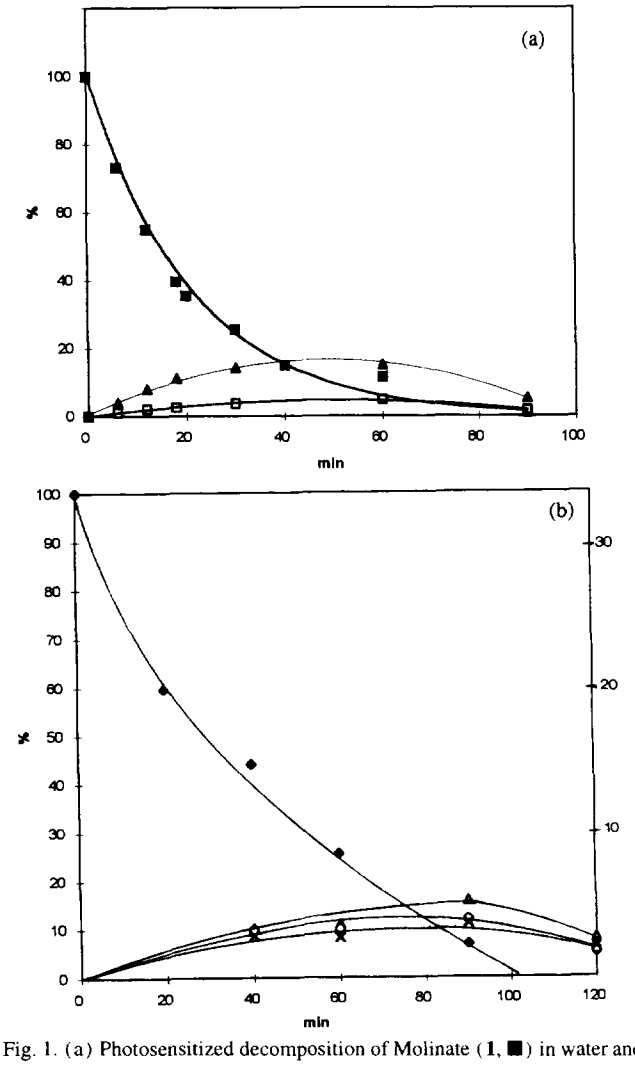

Fig. 1. (a) Photosensitized decomposition of Molinate (**1**, ■) in water and formation of the photoproducts **5** (▲) and **6** (□). (b) Photosensitized decomposition of Eptam (**2**, ♦) in water (left ordinate scale) and formation of the photoproducts **7** (△), **8** (×) and **9** (○) (right ordinate scale).

appreciable photoreaction of the substrates observed when TiO_2 was omitted.

Degradation of Molinate (**1**) was accompanied by the formation of a substantial amount of intermediates (Scheme 1, Table 1). The two main products could be recognized from their mass fragmentation pattern as the 2-azepinone **5** and the 3-azepinone **6** (see Section 5). Further irradiation led to the degradation of these compounds (Fig. 1).

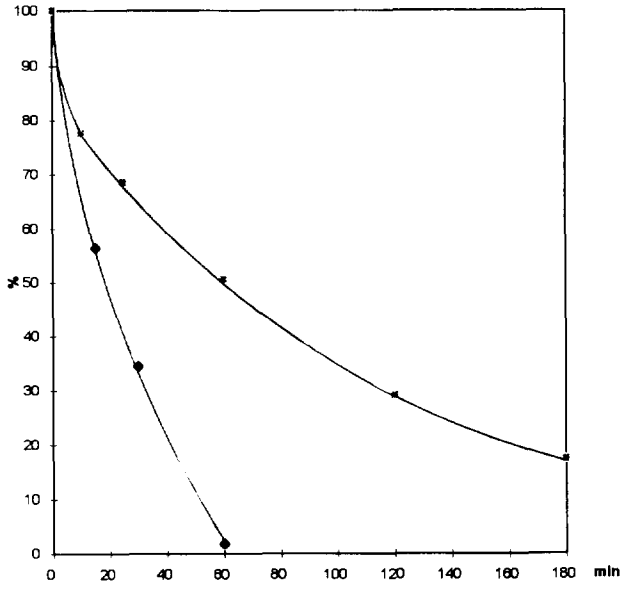

Fig. 2. Photosensitized decomposition of Tiocarbazil (**3**, square) and Thiobencarb (**4**, ♦) in water.

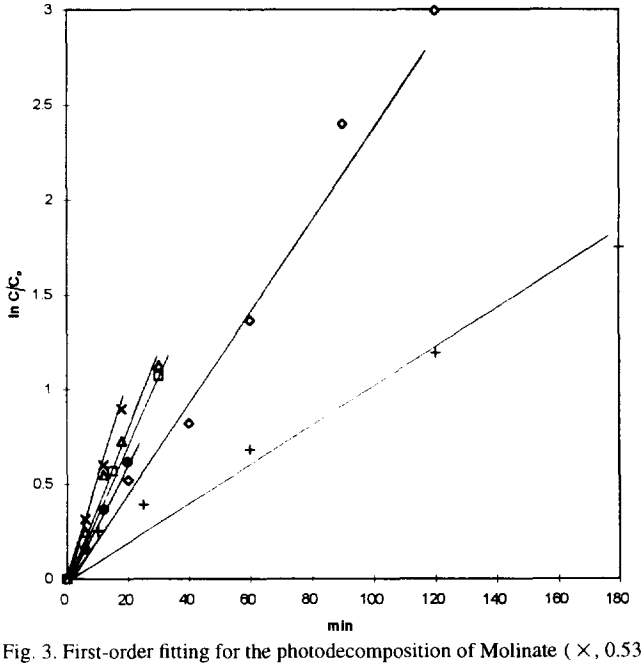

Fig. 3. First-order fitting for the photodecomposition of Molinate (×, 0.53 mM; △, 0.68 mM; ●, 0.90 mM), Eptam (◇, 0.52 mM), Tiocarbazil (+, 0.32 mM) and Thiobencarb (□, 0.37 mM).

Similarly, **2** under these conditions gave several products, recognized as the *N*-formyl- (**7**), *N*-propanoyl- (**8**) and *N*-acetonyl- (**9**) thiocarbamates.

In the case of the thiocarbamates **3** and **4**, both containing an aromatic ring, intermediates were formed only in small amounts. The main intermediates were the corresponding benzaldehydes (**10** and **11** respectively) as well as the imide **12** for the latter substrate.

The decomposition of substrates **1**, **2** and **4** followed apparent first-order kinetics (see Fig. 3). In the case of the benzylthiocarbamate **3**, the reaction was also well fitted by first-order kinetics for the first part, although the substrate

Table 2
Kinetic parameters and quantum yield data for the heterogeneous photosensitized decomposition of thiocarbamates **1–4**

Substrate	k (min^{-1}) [a]	ϕ^a	ϕ^b	k (min^{-1}) [c]
1	5×10^{-2}	0.09	0.12 (7×10^{-4} M)	8×10^{-2}
2	2.5	0.04		
3	2.5	0.028	0.03 (2.5×10^{-4} M)	8
4	3.5	0.04		

[a] Apparent first-order rate constant and quantum yield of substrate decomposition measured at 90 ppm concentration.
[b] Maximum quantum yield measured; the concentration is given in parentheses (see Fig. 4 for the quantum yield dependence on the starting substrate concentration).
[c] Maximum first-order rate constant of substrate decomposition measured at approximately 20 ppm.

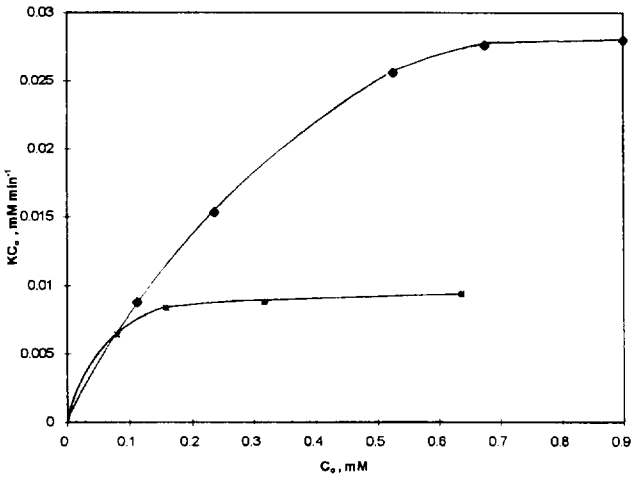

Fig. 4. Dependence of the product kC_0 (proportional to the quantum yield) on the starting concentration C_0 for Molinate (◆) and Tiocarbazil (square).

consumption was slower than expected in the high conversion region. The rate constants for suspensions containing 90 ppm herbicides are reported in Table 2; the quantum yields at the same concentration are also shown. The reactions were examined over a range of concentrations. The amount of substrate consumed increased with increasing concentration up to 100–150 ppm; it then levelled off (see Fig. 4 and the maximum quantum yield in Table 2). Plotting the observed first-order rate of reaction vs. the substrate concentration gave a curved plot (Fig. 4). The maximum rate constants (measured at approximately 20 ppm concentration) are also reported in Table 2.

3. Discussion

3.1. Kinetics

The thiocarbamates studied here are not soluble in water in the range considered, and are adsorbed on the TiO_2 surface. It is generally expected, in view of the fast electron–hole recombination in irradiated semiconductor crystals, that only substrates already adsorbed on the surface have a reasonable probability of reacting, and thus the observed rate is governed by the adsorption kinetics [9]. In the present case, thiocarbamates follow an apparent first-order decomposition rate (see Table 2). The observed decomposition rate constants k are a function of the starting concentration C_0. The reaction quantum yield, which is proportional to the product kC_0, increases with increasing concentration and levels off at approximately 0.3–0.7 mM, namely 100–150 ppm. This fits with the above model of reaction at the surface, but does not prove it. The levelling off of the rate occurs at a value at which monomolecular coverage of the semiconductor surface (50 $m^2\ g^{-1}$, amount used 50 mg per 10 ml) is expected. The substrates are transparent to the wavelengths used, and light is absorbed or reflected by the titania powder. The incident flux was approximately 1×10^{-7} einstein min^{-1} cm^{-2}. We made no correction for light reflection, and the apparent reaction quantum yields reported in Table 2 (values between 0.03 and 0.1) are therefore minimum values, since it is known that loss by scattering is substantial [12]. The rate constants k increase with decreasing initial substrate concentration, and plotting the first-order rate vs. the initial concentration allows the limiting degradation rate to be extrapolated (see Table 2).

3.2. Chemical mechanism

Heterogeneous TiO_2-catalysed photodecomposition of organic substrates is usually assumed [7–11] to occur through the oxidation of water to produce hydroxyl radicals (or some active species on the surface which behaves similarly), with the subsequent reaction of these species with the organic substrate. Alternatively, monoelectronic oxidation of the latter and reaction of the radical cation with oxygen or superoxide anion may take place. In either case, apart from intervening in the chemical process of the primarily formed intermediates, dissolved oxygen plays a key role in intercepting the electron promoted in the conduction band and hence slowing down energy wasting charge recombination within the semiconductor.

The chemistry observed in the present case is fully compatible with the hydroxyl radical path. Thus the detected intermediates are all rationalized as being formed by hydrogen abstraction, followed by the addition of oxygen to the alkyl radical and decomposition of the peroxyl radical formed by C–O or C–C bond cleavage (see Scheme 1). With the aliphatic derivatives, all of the products detected arise from attack at the *N*-alkyl chain. This mainly involves the hydrogens α to the thiocarbamate nitrogen, and leads to acyl and formyl derivatives (products **8** and **7** from **2** from C–O and C–C fragmentation respectively). However, position β also reacts significantly (see products **6** from **1** and **9** from **2**).

The selectivity towards the *N*-alkyl chain is consistent both with chemoselectivity, due to the electrophilic character of the hydroxyl radical, and with steric effects, due to the fact that the substrate is preferentially complexed on the TiO_2 surface through the nitrogen atom, which is the electron-

donating moiety of the molecule. The fact that the selectivity within the chain is moderate, i.e. the ratio for α/β attack is four for **1** and two for **2**, is in favour of the latter mechanism. Indeed, if the intrinsic difference in the reaction rates with $OH^{\cdot}$ in homogeneous solution determines the competition, a much higher preference for abstraction from the weaker α-amino C–H bond vs. the inactivated β C–H bond will be expected. Thus we propose that the molecule is complexed to the semiconductor surface through the nitrogen atom, and this exposes all the hydrogens of the *N*-alkyl chain to the rather unselective attack by surface-bound hydroxyl groups (Scheme 2(a)). Apparently, no competitive oxidation of the *S*-alkyl group takes place, since this is far from the surface.

The aromatic derivatives are also oxidized, although less efficiently. For compound **4**, $OH^{\cdot}$ radical attack at the position α to the nitrogen atom takes place, as positively indicated by the detection of compound **12**. However, attack at the *S*-benzylic position is also an important process, as shown by the identification of the aldehydes **10** and **11** from **3** and **4**. This is expected since homolytic cleavage is easier from a benzylic position. There is no indication that ring hydroxylation, a reaction generally observed with aromatic derivatives under these conditions, occurs here as a primary process, although we cannot exclude the formation and degradation of these derivatives at a rate too high for detection.

The aromatic derivatives **3** and **4** are consumed at a lower rate than **1** and **2**. The apparent quantum yield for the decomposition of the first two compounds is only a few per cent (cf. the values measured for aromatic derivatives [13,14]). Higher values are reached with the aliphatic derivatives (apparent quantum yield, which is a minimum value, of over 10% with **1**). This suggests that the aromatic ring functions as an alternative site for complexation at the semiconductor surface, but reaction of the hydroxyl radicals is less efficient in this case. Complexation through the nitrogen atom and reaction at the *N*-alkyl chain continues (see **12** from **4**), but is slowed down due to the above competition (Scheme 2(b)).

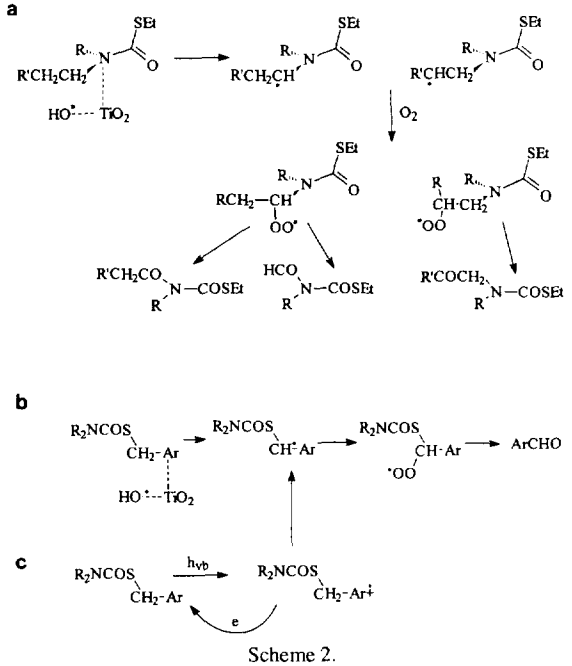

Scheme 2.

In turn, complexation may facilitate the otherwise kinetically prohibited [15] hole transfer to the easily oxidized aromatic ring ($E_{OX} = 2.3$ V vs. saturated calomel electrode (SCE) in MeCN). Deprotonation from the benzylic position then leads to the same radical as above, but this chemical reaction competes with back electron transfer (Scheme 2(c)). The possibility that aromatic derivatives react inefficiently due to a short-circuit reaction (hole transfer followed by back electron transfer) has been pointed out [16]. When there is no alternative, as with the aliphatic thiocarbamates, the efficiency is higher, since electron transfer does not interfere with adsorption and hydrogen abstraction. It should be pointed out, however, that a lower efficiency is observed at high coverage of the semiconductor. The limiting rates at low starting concentration, and thus low surface coverage, are equal for **1** and **3**. It is possible that the two mechanisms have different requirements for the complexation distance and position.

4. Conclusions

This work shows that heterogeneous titanium dioxide-photocatalysed decomposition is a viable pathway for the removal of thiocarbamate herbicides from agricultural effluents. With a small amount of sensitizer (0.5 g l^{-1}) and a UVA flux of 1×10^{-7} einstein min^{-1} cm^{-2}, comparable with that of solar light, concentrations up to 150 ppm are efficiently photodegraded, and no persistent intermediate accumulates in a sizeable amount. The process is rationalized as hydrogen abstraction by surface-bound hydroxyl radicals occurring preferentially on the *N*-alkyl chain. This is an efficient process, resulting in rapid decomposition, particularly in the case of aliphatic thiocarbamates.

5. Experimental details

5.1. General

The thiocarbamates **1–4** were samples of commercial origin. Titanium dioxide (Degussa P25), a known mixture of 80% anatase and 20% rutile with an average particle size of 30 nm and a reactive surface area of approximately 50 m^2 g^{-1}, was used as received. Gas chromatography (GC) analyses were carried out using an HP 5890 apparatus with either a 0.5 mm × 10 m semimicro methylsilicone HP5 column or a 0.3 mm × 30 m capillary column, in both cases with a flame ionization detector (FID). Gas chromatography/mass spectrometry (GC/MS) determination was performed using an HP 5970B instrument operating at an ionizing voltage of 70

eV, connected to an HP 5890 instrument equipped with a 0.2 mm × 25 m capillary column.

5.2. Photocatalysed decomposition

Irradiations were carried out on mechanically stirred, air-equilibrated solutions contained in 4.5 cm diameter beakers. Samples (10 ml) containing 5 mg TiO_2 were used. The suspension was stirred for 10 min, and then irradiated using two 15 W phosphor-coated lamps (centre of emission, 360 nm). The photolysed solution was extracted with 2 × 3 ml CH_2Cl_2, filtered with a 0.45 μm porosity filter under vacuum and rotary evaporated. The residue was dissolved in MeCN (0.5 ml total volume, containing 2,3-dimethylnaphthalene as internal standard) and analysed by GC.

The aldehydes **10** and **11** were recognized by comparison with authentic samples. The identification of the other compounds was based on GC/MS data (see below, peaks with $m/e > 10\%$ or otherwise diagnostic are reported).

S-Ethyl ester of 1-hexahydroazepin-2-one-1-carbamothioic acid (**5**): $T_r = 5.79$ min; *m/e* 201 (11), 178 (15), 140 (28), 112 (100), 98 (16), 84 (15). *S*-Ethyl ester of 1-hexahydroazepin-3-one-1-carbothioic acid (**6**): $T_r = 5.48$ min; *m/e* 201 (14), 178 (15), 140 (28), 112 (100), 98 (16), 84 (15). The main fragmentation paths are identical; the two compounds are distinguished on the basis of the greater polarity, and thus higher T_r, of compound **5**.

S-Ethyl ester of *N*-formyl-*N*-propylcarbamothioic acid (**7**): $T_r = 3.27$ min; *m/e* 175 (3), 146 (14), 119 (23), 114 (14), 89 (18), 86 (23), 72 (14), 62 (100), 61 (23). *S*-Ethyl ester of *N*-propanoyl-*N*-propylcarbamothioic acid (**8**): $T_r = 4.52$ min; *m/e* 203 (3), 160 (63), 146 (10), 132 (100), 90 (11), 89 (92). *S*-Ethyl ester of *N*-(2-oxopropyl)-*N*-propylcarbamothioic acid (**9**): $T_r = 4.17$ min; *m/e* 203 (1), 174 (2), 142 (2), 118 (8), 89 (1), 61 (2), 57 (100). Isomeric **8** and **9** are clearly distinguished by the fragmentation pattern (e.g. strong peaks at 160 ($M - C_3H_7$) and 132 ($M - C_3H_7 - C_2H_4$) in the former case; base peak 57 (CH_3COCH_2) in the latter).

S-(4-Chlorophenylmethyl) ester of *N*-ethanoyl-*N*-ethylcarbamothioic acid (**12**): $T_r = 8.24$ min; *m/e* 271 (32)*, 157 (33)*, 146 (100), 125 (87)*, 100 (10), 89 (22) (asterisks indicate chlorinated fragments).

The substrates are transparent to the wavelength range, and blank experiments showed that no measurable decomposition of the substrates took place when TiO_2 was omitted. The apparent quantum yields reported in Table 2 were calculated using the total incident flux, with no correction for the loss due to scattering. The incident flux was measured by ferrioxalate actinometry.

Acknowledgements

Partial support of this work by MURST is gratefully acknowledged. M.S. and A.C. thank Fondazione Lombardia per l'Ambiente for a fellowship.

References

[1] R.D. Ross and D.G. Crosby, *Environ. Toxicol. Chem., 4* (1985) 773.
[2] J.M. Carrasco, C. Sabater, J.L. Alonso, J. Gonzalez, S. Botella, I. Amoros, M.J. Ibanez, H. Boira and J. Ferrer, *Sci. Total Environ., 123* (1992) 219.
[3] L.O. Ruzo and J.E. Casida, *J. Agric. Food Chem., 33* (1985) 272.
[4] W.M. Draper and D.G. Crosby, *J. Agric. Food Chem., 32* (1984) 231.
[5] W.M. Draper and D.G. Crosby, *J. Agric. Food Chem., 32* (1984) 728.
[6] W.M. Draper, *ACS Symp. Ser., 327* (1987) 268.
[7] P. Pichat, *Catal. Today, 19* (1994) 313.
[8] A. Mills, R.H. Davies and D. Worsley, *Chem. Soc. Rev., 22* (1993) 417.
[9] M.R. Hoffmann, S.T. Martin, W. Choi and D.W. Bahnemann, *Chem. Rev., 95* (1995) 69.
[10] D. Bahnemann, J. Cunningham, M.A. Fox, E. Pelizzetti, P. Pichat and N. Serpone, in G.R. Helz, R.G. Zepp and D.G. Crosby (eds.), *Aquatic and Surface Photochemistry*, Lewis, Boca Raton, FL, 1994, p. 261.
[11] D.F. Ollis, E. Pelizzetti and N. Serpone, in N. Serpone and E. Pelizzetti (eds.), *Photocatalysis*, Wiley, New York, 1989, p. 603. O. Legrini, E. Oliveros and A.M. Braun, *Chem. Rev., 93* (1993) 671.
[12] V. Augugliaro, M. Schiavello and L. Palmisano, *Coord. Chem. Rev., 125* (1993) 173. M. Schiavello, V. Augugliaro and L. Palmisano, *J. Catal., 127* (1991) 132.
[13] J.R. Bolton, *EPA Newsletter*, (1991) 40.
[14] G. Mills and M.R. Hoffmann, *Environ. Sci. Technol., 27* (1993) 1681.
[15] N. Serpone, D. Lawless, R. Khairutdinov and E. Pelizzetti, *J. Phys. Chem., 90* (1993) 16 655.
[16] W. Choi and M.R. Hoffmann, *Environ. Sci. Technol., 29* (1995) 1646.